

DR. KAREN LOUISE THOMSEN (Orcid ID : 0000-0002-8118-4643)

DR. JORDI GRACIA-SANCHO (Orcid ID : 0000-0001-7736-4089)

Article type : Original

Ammonia scavenging prevents progression of fibrosis in experimental non-alcoholic fatty liver disease

Francesco De Chiara^{1†}, Karen Louise Thomsen^{2†}, Abeba Habtesion¹, Helen Jones¹, Nathan Davies¹, Jordi Gracia-Sancho³, Nicolò Manicardi³, Andrew Hall¹, Fausto Andreola¹, Hannah L Paish⁴, Lee H Reed⁴, Abigail A Watson⁴, Jack Leslie⁴, Fiona Oakley⁴, Krista Rombouts¹, Rajeshwar Prosad Mookerjee¹, Jelena Mann⁴, Rajiv Jalan^{1*}

†Joint first authors

*Corresponding author

¹ UCL Institute of Liver and Digestive Health, University College London, United Kingdom

² Department of Hepatology & Gastroenterology, Aarhus University Hospital, Denmark

³ Liver Vascular Biology Research Group, IDIBAPS Biomedical Research Institute & CIBEREHD, Barcelona, Spain

⁴ Newcastle Fibrosis Research Group, Institute of Cellular Medicine, Faculty of Medical Sciences, Newcastle University, Newcastle upon Tyne, United Kingdom

Keywords: ammonia; fibrosis; non-alcoholic fatty liver disease; urea cycle

FOOTNOTE PAGE

Contact information:

Professor Rajiv Jalan

UCL Institute of Liver and Digestive Health

University College London

This article has been accepted for publication and undergone full peer review but has not been through the copyediting, typesetting, pagination and proofreading process, which may lead to differences between this version and the Version of Record. Please cite this article as doi: 10.1002/hep.30890

This article is protected by copyright. All rights reserved.

Royal Free Campus
Rowland Hill Street
London NW32PF
United Kingdom
Phone (direct): +44 2074332795
E-mail: r.jalan@ucl.ac.uk

List of abbreviations:

ALT: alanine aminotransferase
 α -SMA: alpha smooth muscle actin
AST: aspartate aminotransferase
CCl2: chemokine (C-C motif) ligand 2
CPA: collagen proportionate area
CPS1: carbamoyl phosphate synthetase
Col1A1: collagen type I alpha 1
FFAs: free fatty acids
H&E: hematoxylin-eosin
HFHC: high-fat, high-cholesterol
HSCs: hepatic stellate cells
IL: Interleukin
KCs: Kupffer cells
LDH: lactate dehydrogenase
NAFLD: non-alcoholic fatty liver disease
NASH: non-alcoholic steatohepatitis
NC: normal chow
OP: ornithine phenylacetate
OTC: ornithine transcarbamylase
PAG: phenylacetyl glycine
PAGN: phenylacetyl glutamine
PSR: Picro Sirius Red
PCLS: precision cut liver slices
SFM: serum free medium
TIMP1: metalloproteinase inhibitor 1
TLR4: toll-like receptor 4
UCEs: urea cycle enzymes
WB: western blots

Financial support:

This study was generously supported by grants from the Novo Nordisk foundation, the Danish Council for Independent Research, Instituto de Salud Carlos III - Ministerio de Ciencia, Innovación y Universidades (FIS P117/00012) and through an unrestricted grant from Ocera Therapeutics.

ABSTRACT

In non-alcoholic fatty liver disease (NAFLD), fibrosis is the most important factor contributing to NAFLD-associated morbidity and mortality. Prevention of progression and reduction in fibrosis is the main aim of treatment. Even in early stages of NAFLD, hepatic and systemic hyperammonaemia is evident. This is due to reduced urea synthesis and as ammonia is known to activate hepatic stellate cells, we hypothesised that ammonia may be involved in the progression of fibrosis in NAFLD. In a high-fat high-cholesterol diet induced rodent model of NAFLD, we observed a progressive step-wise reduction in the expression and activity of urea cycle enzymes resulting in hyperammonaemia, evidence of hepatic stellate cell activation and progressive fibrosis. In primary, cultured hepatocytes and precision cut liver slices we demonstrated increased gene expression of pro-fibrogenic markers after lipid and/or ammonia exposure. Lowering of ammonia with the ammonia scavenger ornithine phenylacetate (OP) prevented hepatocyte cell death and significantly reduced the development of fibrosis both *in vitro* in the liver slices and also *in vivo* in the rodent animal model. The prevention of fibrosis in the rodent model was associated with restoration of urea cycle enzyme activity and function, reduced hepatic ammonia and markers of inflammation. *Conclusion:* The results of this study suggest that hepatic steatosis results in hyperammonaemia, which is associated with progression of hepatic fibrosis. Reduction of ammonia levels prevented progression of fibrosis providing a potentially novel treatment for NAFLD.

Due to alarming increases in obesity in the industrialised countries, non-alcoholic fatty liver disease (NAFLD) is now the most widely recognized cause of liver dysfunction, cirrhosis and an indication for liver transplantation (1-3). NAFLD is a spectrum of liver diseases ranging from steatosis, through non-alcoholic steatohepatitis (NASH) and cirrhosis. Fibrosis is the key driver of increased morbidity and mortality of patients with NAFLD (4-6) and, prevention of progression and reduction of fibrosis is the main aim of treatment.

In experimental models of NAFLD, gene and protein expression of mitochondrial urea cycle enzymes carbamoyl phosphate synthetase (CPS1) and ornithine transcarbamylase (OTC) are reduced significantly, resulting in reduced ureagenesis and hyperammonaemia (7-9). This is reversible upon recovery from NAFLD. Also in non-cirrhotic patients with NAFLD, a reduction in urea cycle enzymes (UCEs) and, at the same time, increased plasma and hepatic ammonia levels was observed (8, 9).

Hyperammonaemia produces numerous deleterious effects in liver disease patients, ranging from hepatic encephalopathy to neutrophil dysfunction and sarcopenia (10-13). Ammonia has been shown to activate human hepatic stellate cells (HSCs) *in vitro* and *in vivo* (14). HSCs are key cells involved in the progression of hepatic fibrosis and changes from a quiescent to an activated state in conditions of hepatocellular injury enabling them to participate in the wound healing process (15). Reduction of ammonia concentrations with the ammonia scavenger ornithine phenylacetate (OP) prevented the activation of HSCs and reduced the severity of portal hypertension in an animal model of advanced liver fibrosis (14). Therefore, hyperammonaemia-induced activation of HSCs may favour the progression of fibrosis

in NAFLD and ammonia may represent a novel therapeutic target. The ammonia-lowering agent OP modulates interorgan metabolism resulting in a reduction in the severity of hyperammonaemia. OP successfully prevents increases in ammonia in animal models of acute and acute-on-chronic liver failure (16-19) and is a safe and effective ammonia scavenger that is in clinical development to treat hyperammonaemia in patients with cirrhosis (20, 21).

The aims of this study were to investigate the time course of urea cycle dysfunction and the consequent hyperammonaemia in a high-fat, high-cholesterol (HFHC) diet-induced animal model of advanced fibrosis. This study also aimed to determine whether lipids and increased ammonia *in vitro* in hepatic cell cultures and precision cut liver slices promotes fibrogenesis. Finally, this study investigated whether lowering ammonia levels using OP prevented the progression of hepatic fibrosis in the *in vitro* and *in vivo* models.

MATERIAL AND METHODS

UREA CYCLE DYSFUNCTION IN EXPERIMENTAL NAFLD

Animal studies

Study design

The study was performed to determine the time course of urea cycle dysfunction and the consequent hyperammonaemia in a HFHC diet-induced NASH rodent model of advanced fibrosis. The study was conducted in accordance with the UK Animals (Scientific Procedures) Act (1986, revised 2013), following approval from the local animal welfare and ethical review board. Forty-five male Sprague Dawley (SD) rats (body weight 220-250 gr; Charles River, Margate, UK) were divided into nine groups (n=5) and fed normal chow (NC), a high-calorie HC (D12450J, Research Diets, New

Brunswick, NJ, USA) or a HFHC diet (D09052204Y, Research Diets) for 4, 10 or 16 weeks. Please refer to the supplemental material section for more detailed information.

Blood analyses

Plasma ammonia (NH_4^+), alanine aminotransferase (ALT), aspartate aminotransferase (AST), bilirubin, albumin, total cholesterol and triglycerides were measured by a COBAS system (Integra II, Roche UK).

Inflammatory markers

Plasma interleukin (IL)-1 β and IL-10 levels were measured by Luminex assay (R&D Systems, Abingdon, UK) as described in the supplemental material section.

HEK-BlueTM hTLR4 reporter cells

In order to determine whether toll-like receptor 4 (TLR4)-ligands were released into the circulation, plasma was co-incubated with HEK-BlueTM-hTLR4 cells (hkb-htlr4, Invivogen, San Diego, CA, USA) as described in the supplemental material section.

Plasma markers of cell death

An *in vitro* quantitative photometric enzyme immunoassay Cell Death Detection ELISA^{PLUS} (Roche, Basel, Switzerland) was employed to determine histone (H1, H2A, H2B, H3, and H4)-associated DNA (single-stranded and double-stranded) fragments released into the plasma after cell death as described in the supplemental material section.

Liver tissue analyses

Protein expression of markers of fibrosis

Proteins from rat liver tissues were homogenized and the protein content was determined by the microBCA assay kit (Thermo Fisher Scientific, Waltham, MA, USA) as described in the supplemental material section. All liver tissue samples from each group (n=5) were pooled at a final concentration of 30µg/lane.

Proteome Profiler™ Antibody Arrays for cytokines and chemokines

Pooled total liver proteins (mentioned above) were incubated with Proteome Profiler Rat Cytokine Array Kit, Panel A (R&D Systems, Abingdon, UK) as described in the supplemental material section.

Markers of hepatic cell death

In order to assess whether hepatic cell death occurred, TUNEL and histone 3 (H3) staining of the liver tissue was performed. Enzymatic labelling of hepatic cell death was assessed by In Situ Cell Death Detection Kit, POD (Roche, UK). Please refer to the supplemental material section for detailed information.

Ammonia staining

Five µM paraffin embedded sections were dewaxed in xylene and hydrated through graded alcohols. Sections were washed in distilled water and incubated for 5 mins with Nessler's reagent (Sigma-Aldrich, Saint Louis, MO, USA) previously filtered with a 0.45 µM membrane. The sections were then washed briefly twice in distilled water, counterstained with haematoxylin (Sigma-Aldrich, Saint Louis, MO, USA), washed with running tap water, dehydrated in graded alcohol and mounted with DPX permanent mounting medium (22).

OTC enzyme activity

In brief, liver samples were incubated in the presence of excessive amounts of L-ornithine and carbamoyl phosphate under optimal enzyme conditions (triethanolamine solution). Please refer to the supplemental material section for more detailed information.

Immunohistochemistry imaging quantification

TUNEL and H3 immunohistochemistry (IHC) and ammonia staining were quantified using the Open Source Plugin for the Quantitative Evaluation optimised by Varghese et al. (23) as described in the supplemental material section.

Histological analyses and PSR staining

The histology of all the liver specimens was evaluated blindly and scored using the NAS scoring system (NAFLD activity score) (24) as described in the supplemental material section. Fibrosis was measured as collagen proportionate area (CPA) using established techniques (25) on PSR stained sections.

In vitro cell cultures

The study was performed to define the effect of lipid accumulation in hepatocytes on ammonia metabolism and to determine whether the supernatant from these cultured steatotic hepatocytes would induce a fibrogenic signal in HSCs and an inflammatory signal in KCs. All experiments were approved by the Laboratory Animal Care and Use Committee of the University of Barcelona and were conducted in accordance with the European Community guidelines for the protection of animals used for experimental and other scientific purposes (European Economic Community Directive 86/609).

Cell isolation

All cell isolations were performed from female SD rats (n=4, 300-350g) (Charles River, Sant Cugat del Vallès, Spain) as previously described (26, 27). Please refer to the supplemental material section for further information on cell isolation and primary hepatocyte, Kupffer cell (KC) and HSC cultures and treatments.

Supernatant from primary hepatocytes

Ammonia levels were measured using standard methods at the Hospital Clinic of Barcelona's CORE laboratory. Cell Death Detection ELISAPLUS (Sigma-Aldrich) was used to quantify the histone-associated-DNA-fragments according to the manufacturer's protocol.

Real-time qPCR & Western blot analysis

Please refer to the supplemental material section for more detailed information.

EFFECT OF OP IN THE PREVENTION OF PROGRESSION OF HEPATIC FIBROSIS

The ammonia-lowering agent OP (28) (branded as OCR-002) was produced by Ocera Therapeutics (Redwood city, CA, USA) and donated by the company for these experiments.

Precision Cut Liver Slices (PCLS)

This study was conducted in the *in vitro* PCLS model of hepatic steatosis (29) to determine whether progression of fibrosis could be prevented with the ammonia scavenger OP.

Animals

10-14 week old male SD rats (Charles River, Margate, UK) were used in this study. Rats were housed in RC2 cages, with cardboard tubes for environmental enrichment, free access to RM3 diet (DBM diets, Broxburn, UK) and water and maintained on a 12h light/dark cycle.

Lipid treatments

PCLS were generated as described in the supplemental material section (29). PCLS were rested for 24hrs after the cutting, then the first lipid treatment was applied. The free fatty acid (FFA) mix containing oleic, palmitic, linoleic and elaidic acid (final concentration 2mM, based on lipidomic studies performed on serum in NAFLD patients) was conjugated to fatty acid-depleted BSA (final concentration 0.2mM, Sigma). Slices were treated +/- lipid mix for 24hrs before a further 48hr treatment with one of the following treatments; control media plus vehicle, lipids plus vehicle, lipids plus NH_4Cl (100 μm), lipids plus OP (150 $\mu\text{g}/\text{ml}$) or lipids plus NH_4Cl (100 μm) and OP (150 $\mu\text{g}/\text{ml}$). The ammonia dose showed good induction of response without associated toxicity (pilot experiment, not shown). Media was collected and snap frozen every 24hrs for future analysis. Total treatment time with lipids was 96h and treatment time with ammonia and/or OP was 48h. Total experiment time was 5 days (24h initial rest post cutting plus 96h lipid treatment). The groups of lipids plus vehicle and lipids plus NH_4Cl as well as the groups of lipids plus OP and lipids plus NH_4Cl and OP were amalgamated for further analyses.

Albumin, lactate dehydrogenase (LDH) and ammonia quantification in PCLS supernatant

ELISA quantifications for rat albumin (Bethyl laboratories, Cambridge, UK) and rat LDH (Pierce LDH cytotoxicity kit, Thermo Fisher) were performed as per manufacturer's instructions. Ammonia detection was performed by the indophenol direct method (30) as described in the supplemental material section.

RNA isolation, cDNA synthesis and PCR

Two PCLS per condition were collected for RNA extraction; total RNA was purified using the RNeasy Micro Kit (Qiagen, Manchester, UK) following manufacturers instructions as described in the supplemental material section. Experiment was carried out on six separate livers.

Histology

5- μ m-thick PFFE liver sections were processed for PSR staining. Images were acquired at x100 magnification using a Nikon ECLIPSE Ni-U microscope (NIS-Elements Br, Nikon, Kingston upon Thames, UK). The average PSR percentage area was digitally quantified in 10 fields at x100 magnification using Nikon Elements Imaging Software.

In vivo animal studies

Study Design

The study was performed to investigate whether treatment of HFHC animals with the ammonia-lowering agent OP prevents the progression and severity of hepatic fibrosis. 60 male SD rats (body weight 220-250 gr; Charles River, Margate, UK) were

housed and monitored as described above. The animals were divided into six groups (n=10) and fed NC +/- OP, HC diet +/- OP, or HFHC diet +/- OP for 16 weeks using the same diets as described above. OP (Ocera Therapeutics, Redwood city, CA, USA) was mixed into the diets by the manufacturer aiming for a dose of 0.6 g/kg/day. During the last week of the study, rats included were moved into metabolic cages to collect urine over 24 hours. Liver tissue and blood were collected and stored as described above.

Blood analyses

Plasma NH_4^+ , ALT, AST, bilirubin, albumin, total cholesterol and triglycerides as well as plasma IL-1 β and IL-10, HEK-BlueTM hTLR4 reporter cells and histone-associated DNA were measured as described above.

Liver tissue analyses

Protein expression of fibrosis markers, cytokines and chemokines and OTC enzyme activity were measured as described above. TUNEL, histone and ammonia staining of liver tissue and histological analyses were performed and quantified as described above.

Urine analyses

The urine concentrations of phenylacetylglycine (PAG) and phenylacetylglutamine PAGN were measured using liquid chromatography tandem mass spectrometry, based on a modified method that has been previously described (31).

Statistical analysis

Statistical analyses were performed using Stata 14 software (Stata Corporation, College Station, TX). In both *in vitro* studies and animal studies, continuous variables were analysed using Kruskal-Wallis rank test and histology scores using Fisher's exact test when comparing all groups. When significant, post-hoc tests for continuous variables were performed among groups by the Mann-Whitney test and histology scores using Fisher's exact test. Data are presented as median (IQR). P-values <0.05 were considered statistically significant.

RESULTS

Progressive urea cycle dysfunction and hyperammonaemia in a NAFLD animal model and a cellular model of steatosis

Animal Model

In order to define the time course and the relationship between progression of NAFLD, dysfunction of UCEs and consequent hyperammonaemia, we studied rodents fed with NC, HC and HFHC diet. The animals were terminated after 4, 10 and 16 weeks during which they displayed evidence of progressive fibrosis. Body weight increased in the animals in all groups and no significant differences in body weight increments were observed between the groups from 4 weeks and onwards, *Suppl. Figure 1A*. However, the liver to body weight ratio increased significantly more in the animals in the HFHC diet group compared with the HC diet and NC groups at all time points under investigation, *Table 1*. This was associated with increases in alanine ALT and AST in the HFHC animals compared with NC animals with the highest levels observed after 10 weeks. Also, plasma total cholesterol levels were increased in HFHC animals compared with the HC and NC animals, *Table 1*.

Macroscopically, the livers from HC and HFHC diet animals were progressively enlarged compared to NC animals (21 (19-22), 36 (33-38) g vs. 17(15-18) g at 16 weeks, $P=0.003$), *Suppl. Figure 1B & Table 1*. Microscopically, the HC livers showed moderate macrovesicular steatosis at 16 weeks but the HFHC livers showed severe, predominantly microvesicular steatosis, inflammatory infiltrates and massive ballooning of hepatocytes. Also, expanded portal tracts, perisinusoidal fibrosis and borderline bridging fibrosis were observed, *Figure 1A & Table 1*. The whole-slide digital quantification of PSR and polarized light confirmed the increased collagen deposition in HFHC at 10 and 16 weeks compared with NC and HC diet groups (6.5 (5.5-11.7)% vs. 1.2 (0.6-1.3)% and 2.0 (1.9-2.3)%, respectively at 16 weeks; $p<0.01$), *Figure 1A & B*. The HFHC diet induced an increase in protein levels of collagen type I alpha 1 (Col1A1) and Myosin IIa at all time points and at 16 weeks also in Myosin IIb and alpha smooth muscle actin (α -SMA) levels compared with NC indicating activation of HSCs, *Figure 1C*. The HC diet also increased Col1A1 and Myosin IIa levels at 16 weeks compared to NC, *Figure 1C*. Furthermore, a proteome array displayed an increase in metalloproteinase inhibitor 1 (TIMP1) in HFHC-fed animals in a time-dependent manner and also in the HC animals at 16 weeks compared with NC, *Suppl. Figure 1C*.

OTC activity decreased progressively in both HFHC and HC-fed animals compared with NC animals (0.19 (0.18-0.22) and 0.39 (0.38-0.40), respectively vs. 0.51 (0.49-0.52) nmol/min/ μ g protein at 16 weeks; $p<0.01$, both), *Figure 1D*. Also, the HFHC diet, but not the HC diet, increased plasma ammonia levels at 10 and 16 weeks compared with NC (188 (186-195) vs. 66 (51-77) μ mol/L at 10 weeks; $p<0.01$), *Figure 1E*. Moreover, Nessler's staining confirmed the presence of high levels of ammonia

(brown precipitates) in the liver of HFHC group compared with NC and HC at 16 weeks, *Figure 1F*. Taken together, these data provided *in vivo* evidence of progressive hyperammonaemia, which correlated with the severity of hepatic fibrosis during evolution of injury and fibrosis in the HFHC group.

Plasma IL-1 β and IL-10 were increased in HFHC animals compared with HC and NC animals from 10 weeks onwards providing evidence of systemic inflammation *Suppl. Figure 1D*. In the liver tissue, an increase in protein levels of CINC-1, fractalkine and sICAM in HFHC animals indicated simultaneous hepatic inflammation, *Suppl. Figure 1C*. Plasma histone (H)-associated DNA fragments increased in HFHC animals at 10 and 16 weeks compared with NC, *Figure 1G*. Moreover, the vast majority of hepatocyte nuclei showed positive H3 staining (>95%) in the HFHC livers providing evidence of hepatocyte cell death, whereas NC-fed animals only demonstrated slight H3 staining lining the hepatocytes, *Suppl. Figure 1E*. TUNEL staining of the liver tissue showed nuclear positivity of hepatocytes (>50%) both in HC and HFHC animals compared with only a few positively stained hepatocyte nuclei in NC. The staining in the HFHC-fed animals was more frequent in the cytoplasm (<10%) compared to HC-fed animals (<1%) ($p < 0.01$), *Figure 1H*. This was associated with increased presence of TLR4-ligands in plasma of HFHC animals compared with NC and HC at 16 weeks ($p < 0.01$, both), *Suppl. Figure 1F*.

Cellular Model

In order to define the effect of lipid accumulation in hepatocytes on UCE function and ammonia metabolism, an *in vitro* model of hepatocyte steatosis was developed by incubating primary hepatocytes with FFAs for 48h and 72h (9). *Figure 2A* shows

accumulation of lipid droplets intracellularly. An increase in ammonia, *Figure 2B*, and cell death components in the medium and a decrease in DNA yields after lysis, *Suppl. Figure 2A*, were observed. The mean ammonia concentration in the supernatant after incubation with 200 μ M FFAs for 48h was 212 ± 16 μ M. Therefore, an ammonia dose of 200 μ M was used for the subsequent treatment of HSCs and KCs. As steatotic hepatocytes are in close proximity to the HSCs and KCs, further studies were performed to determine whether the supernatant from the cultured steatotic hepatocytes (48h) would induce a fibrogenic signal in HSCs and an inflammatory signal in KCs. The HSCs were treated with serum free medium (SFM), FFAs (200 μ M), ammonia (200 μ M) or the supernatant from FFA-treated hepatocytes for 72h and left to recover for another 72h. Increased proliferation and metabolic activity of HSCs treated with ammonia and the hepatocyte supernatant was observed, *Figure 2C*, *Suppl. Figure 2B* compared with SFM- and FFA-treated cells, showing rapid intracellular accumulation of lipids in the latter, *Suppl. Figure 2C*. The hepatocyte supernatant induced the formation of HSC clusters, *Figure 2C*. Furthermore, ammonia and hepatocyte supernatant treatment increased the α -SMA and Col1A1 HSC mRNA levels compared with the control SFM- and FFA-treated cells, *Figure 2D*. In addition, α -SMA and Col1A1 protein levels were increased by ammonia and hepatocyte supernatant treatment as demonstrated by western blots (WB) (*Figure 2E*), and by α -SMA fluorescence staining (*Figure 2F*). Replacing the FFA-, ammonia- or supernatant-containing medium with SFM for another 72h led to an amelioration in HSCs phenotype (*Figure 2C-F*). Freshly isolated KCs were incubated for 24h with SFM, FFAs (200 μ M), ammonia (200 μ M) or hepatocyte supernatant. KCs treated with ammonia and supernatant exhibited flat amoeboid morphology with extended filopodia and lamellipodia, *Figure 2G*. Interestingly, FFAs, ammonia and hepatocyte

supernatant induced an increase in mRNA level of IL1b and chemokine (C-C motif) ligand 2 (CCL2), whereas ammonia and the hepatocyte supernatant increased also IL-6 levels ($p=0.06$, all) *Figure 2H*. These *in vitro* studies in isolated cells provided direct evidence that steatotic hepatocytes have higher ammonia in the culture supernatants that is able to induce the activation of HSCs and KCs.

Prevention of progression of hepatic fibrosis in PCLS and a NAFLD animal model after treatment with the ammonia scavenger, OP

PCLS model

We then determined whether progression of fibrosis could be prevented with an ammonia scavenger in a validated *in vitro* model of hepatic steatosis (32). Media albumin and LDH concentrations were measured during the time course of the experiments to validate the functional status and viability of the PCLS, *Figure 3A*. The ammonia levels in the culture medium increased with lipid and ammonia treatment ($p=0.0001$), *Figure 3B*. Adding OP to the culture medium decreased the ammonia levels in the medium of the lipid- and/or ammonia-treated liver slices both after 24h ($p=0.002$) and also 48 h ($p<0.001$), *Figure 3B*. Lipid and/or ammonia treatment of the liver slices increased the gene expression of α -SMA ($p=0.04$) and Col1A1 ($p=0.05$) compared with untreated control liver slices, *Figure 3C*. Adding OP to the lipid- and/or ammonia-treated liver slices for 48 hours reduced the gene expression of Col1A1 ($p=0.03$) and tended to reduce the gene expression of α -SMA ($p=0.13$), *Figure 3C*. Treatment with lipids and/or ammonia increased the collagen deposition in the liver slices, defined by PSR staining, which was reduced in the liver slices that were treated with OP ($p=0.04$), *Figure 3D*, providing proof of concept that reducing ammonia reduced the severity of fibrosis in this *in vitro* model.

Animal model

In order to validate the effect of targeting ammonia on the progression of fibrosis, we administered OP to the HC and HFHC animals. No differences in body weight were observed in the groups treated with OP compared with the respective untreated groups, *Table 2*. However, OP decreased the liver to body weight ratio in all groups, *Table 2*. OP treatment had no effect on liver biochemistry or lipids in any of the groups, *Table 2*.

OP treatment significantly increased the OTC activity in HFHC animals (0.32 (0.29-0.36) vs. 0.22 (0.19-0.28) nmol/min/ μ g protein, $p=0.01$), but had no such effect in HC animals, *Figure 4A*. OP tended to decrease plasma ammonia levels in the HFHC group compared with non-treated animals (76 (67-96) vs. 119 (80-169) μ mol/L, $p=0.07$), *Figure 4B*, and a significant decrease was observed in the liver tissue using Nessler's staining (2173 (1785-2635) vs. 3185 (2985-3266), $p=0.004$), *Figure 4C*. This was associated with a significant increase in urinary PAG and PAGN concentrations in the OP-treated animals demonstrating the delivery of effective concentrations of OP to the treated groups, *Figure 4D*. A minor increase in PAG and PAGN was also observed in the non-treated HFHC animals, which is likely due to the presence of phenylbutyric acid in the HFHC diet.

In the plasma, OP reduced IL-1 β (30 (18-46) vs. 341 (300-420) pg/mL, $p=0.0002$) and IL-10 (79 (65-89) vs. 115 (100-131) pg/mL, $p=0.007$) levels in the HFHC animals compared with the untreated animals, *Figure 4E*. Furthermore, a significant decrease in plasma TLR4-ligands was observed in the OP-treated HFHC group compared with the untreated group (0.51 (0.43-0.67) vs. 0.96 (0.73-1.07), $p=0.005$), *Figure 4F*. In the

liver tissue, OP treatment led to a reduction in the protein levels of sICAM in the HC and HFHC animals compared with the untreated groups, *Suppl. Figure 3A*. OP treatment tended to decrease the levels of cell death components in plasma in HFHC animals compared with untreated animals ($p=0.14$), *Figure 4G*. Also in liver tissue, a tendency to a reduction in H3 staining was observed after OP treatment in HFHC animals ($p=0.13$), *Suppl. Figure 3B* and TUNEL staining was significantly decreased by OP with less nuclear positivity of hepatocytes (<25%) in HFHC animals compared with the untreated group (<50%) ($p=0.007$), *Figure 4H*.

Macroscopically, the liver from the HFHC animals after 16-weeks of OP treatment was less steatotic compared with the untreated HFHC animals. Microscopically, the OP-treated HFHC animals showed less necrotic foci and fibrosis, *Figure 4I, Suppl. Figure 3C & Table 2*. Fibrosis quantification was performed by whole liver histologic slide analysis showing decreased fibrosis in OP-treated HFHC animals ($p=0.007$), *Figure 4I*. This was associated with reduced hepatic expression of Col1A1, Myosin IIa, Myosin IIb and α -SMA and TIMP1 levels in HFHC animals indicating less activation of HSCs, *Figure 4J & Suppl. Figure 3A*. These data confirmed that OP significantly reduced the progression of fibrosis in the HFHC animals.

DISCUSSION

The main results of this study show for the first time evidence of progressive hyperammonaemia in an animal and cellular model of NAFLD, which was associated with progressive reduction in the expression and function of the mitochondrial urea cycle enzyme, OTC. The pathophysiological significance of the steatosis-associated hyperammonaemia was defined using supernatants of isolated primary steatotic hepatocytes and their ability to induce cytokine gene expression in KCs and activate

fibrogenic pathways in HSCs. This effect of steatosis-induced hyperammonaemia and associated fibrosis was reproduced in the PCLS model. Most importantly, the results provide evidence that reducing ammonia may be a novel approach to the prevention of progression of NAFLD by demonstrating that an ammonia scavenger, OP, was able to prevent the progression of fibrosis in the PCLS model and the animal model, *Figure 5*.

Initially, we investigated the urea cycle enzyme function longitudinally at different time points in NC animals and during progression of NAFLD in the rodent model to determine the time course of changes in the severity of fibrosis and ammonia metabolism. In control animals, we observed a slight decrease in OTC enzyme activity over time. This phenomenon has been previously described with increasing age (33). Although both HC and HFHC-fed animals demonstrated reduced OTC enzyme activity even in early disease, this was substantially more marked in the HFHC animals and ammonia levels were increased only in HFHC animals and not in the HC diet animals. This observation of reduced OTC activity and hyperammonaemia is in accordance with a recent study from our group in experimental and human NAFLD (9), where we confirmed that the underlying mechanism was the methylation of the OTC gene. This was associated with increased expression of pro-fibrogenic proteins and progressive fibrosis was only observed in the HFHC-fed animals. These findings support our previous observation of hyperammonaemia promoting activation of HSCs and fibrosis (14). However, markers of hepatocyte cell death were observed both in the hepatic extracellular space and also in the systemic circulation in both HC and HFHC-fed animals. Cell death components such as damage-associated molecular patterns (DAMPs) can

initiate and perpetuate an inflammatory response (34, 35). However, despite high levels of cell death components in HC animals, they did not induce an increase in inflammatory markers or fibrosis compared with the HFHC animals. This observation supports our hypotheses that steatosis-induced hyperammonaemia may be an important driver of the pro-fibrogenic response.

We used two different *in vitro* models of steatosis to confirm the potential role of ammonia in inducing fibrosis. In primary rat hepatocytes, induction of hepatocyte steatosis increased ammonia concentration in the supernatant fluid indicating dysfunctional urea synthesis as previously described (9). In the HSC and KC cultures, both ammonia and the supernatant from the primary steatotic hepatocytes were able to activate the respective cells as was demonstrated by increased pro-fibrogenic gene expression in HSCs and markers of inflammation in KCs. However, the supernatant most likely also contained other pro-fibrotic substances released from the hepatocytes such as DAMPs, reactive oxygen species (ROS) and pro-fibrotic cytokines, which could activate the cells. It is important to note that treatment of neither KCs nor HSCs with lipids produced this effect. Replacing the media with fresh serum free media restored the observed changes in the HSCs demonstrating reversibility. Similar reversibility has been shown in our previous studies where restoring the diet of HFHC animals after 10 months to normal chow for 2 months was associated with partial restoration in the activity of the UCEs. These data were confirmed in the PCLS model, which has the advantage of having all the parenchymal and non-parenchymal cells intact. Induction of steatosis and addition of ammonia to the medium increased the gene expression of pro-fibrogenic markers and hepatic fibrosis.

Having shown the potential role of ammonia in the pathogenesis of NAFLD progression, we explored whether ammonia may indeed be a therapeutic target for treatment of patients with NAFLD. We chose to use a novel ammonia scavenger that is currently in clinical trials for the treatment of hepatic encephalopathy, OP, which has been shown to use redundant pathways involved in ammonia metabolism to reduce ammonia in patients with cirrhosis and acute liver failure. The efficacy of OP is based on the capacity of ornithine to increase the formation of glutamine. The newly formed glutamine combines with phenylacetate, allowing the removal of ammonia by its conversion into PAGN (16, 36). In the PCLS model of hepatic steatosis described above, the addition of OP to the supernatant reduced ammonia concentrations and normalized the genetic markers of fibrogenesis and tended to reduce the severity of fibrosis. We confirmed these results obtained in the *in vitro* model in the HFHC animals and treated them with OP from the time of onset of the HFHC diet. Ammonia levels were significantly reduced in the liver in the HFHC animals and a tendency to reduction in plasma ammonia was observed in the HFHC animals treated with OP with a concomitant increase in urinary metabolites. This reduction of ammonia in HFHC animals was associated with a significant reduction in cell-death markers in both plasma and liver tissue and reduction in the concentration of TLR4-ligands and cytokines in plasma. Most importantly, we observed a significant reduction in the markers of HSC activation and hepatic fibrosis demonstrating that the ammonia-lowering agent OP effectively prevents progression of fibrosis.

Accepted Article

It is possible that a part of this OP effect may be due to its effects on reduction of cell death through reduction of ammonia. Many studies support the notion that ammonia is more than a neurotoxin as it has been shown to exert direct hepatotoxicity, produce deleterious effect on neutrophil function and is important in the pathogenesis of sarcopenia observed in liver failure (13). Although the HC and HFHC animals were both fed diets with high calorie content, total body weight was similar in all three groups after 4 weeks and up to 16 weeks when the study was terminated. Moreover, the livers of the HC and HFHC animals were significantly enlarged. Therefore, it seems reasonable to think, that the HC and HFHC-fed rats probably suffered from sarcopenia in line with previous findings in human NASH (37), which was probably ameliorated by OP treatment manifested as a reduction in the liver to body weight ratio while the liver weight remained unchanged. This hypothesis will need to be confirmed in future studies.

In conclusion, steatosis in rats and in *in vitro* models was associated with progressive urea cycle dysfunction resulting in hyperammonaemia and progressive hepatic fibrosis. The ammonia scavenger, OP prevented the development of hyperammonaemia and progression of fibrosis both *in vitro* and *in vivo* models of NAFLD. Taken together, these data suggest that ammonia may be a target for the prevention of progression of fibrosis and provides the rationale for clinical application.

ACKNOWLEDGEMENTS

We thank Ole Martin Fuskevåg, University Hospital of North Norway, Tromsø, Norway for performing urine PAG and PAGN analyses.

REFERENCES

1. Hardy T, Anstee QM, Day CP. Nonalcoholic fatty liver disease: new treatments. *Current Opinion in Gastroenterology* 2015;31:175-183.
2. Blachier M, Leleu H, Peck-Radosavljevic M, Valla DC, Roudot-Thoraval F. The burden of liver disease in Europe: a review of available epidemiological data. *J Hepatol* 2013;58:593-608.
3. Wang Y, Beydoun MA, Liang L, Caballero B, Kumanyika SK. Will all Americans become overweight or obese? estimating the progression and cost of the US obesity epidemic. *Obesity (Silver Spring)* 2008;16:2323-2330.
4. Ekstedt M, Hagstrom H, Nasr P, Fredrikson M, Stal P, Kechagias S, et al. Fibrosis stage is the strongest predictor for disease-specific mortality in NAFLD after up to 33 years of follow-up. *Hepatology* 2015;61:1547-1554.
5. Angulo P, Kleiner DE, Dam-Larsen S, Adams LA, Bjornsson ES, Charatcharoenwitthaya P, et al. Liver Fibrosis, but No Other Histologic Features, Is Associated With Long-term Outcomes of Patients With Nonalcoholic Fatty Liver Disease. *Gastroenterology* 2015;149:389-397 e310.
6. Hagstrom H, Nasr P, Ekstedt M, Hammar U, Stal P, Hultcrantz R, et al. Fibrosis stage but not NASH predicts mortality and time to development of severe liver disease in biopsy-proven NAFLD. *J Hepatol* 2017;67:1265-1273.
7. Thomsen KL, Gronbaek H, Glavind E, Hebbard L, Jessen N, Clouston A, et al. Experimental nonalcoholic steatohepatitis compromises ureagenesis, an essential hepatic metabolic function. *American Journal of Physiology. Gastrointestinal and Liver Physiology* 2014;307:G295-301.
8. Thomsen KL, De Chiara F, Rombouts K, Vilstrup H, Andreola F, Mookerjee RP, et al. Ammonia: A novel target for the treatment of non-alcoholic steatohepatitis. *Med Hypotheses* 2018;113:91-97.
9. De Chiara F, Heeboll S, Marrone G, Montoliu C, Hamilton-Dutoit S, Ferrandez A, et al. Urea cycle dysregulation in non-alcoholic fatty liver disease. *J Hepatol* 2018;69:905-915.
10. Clemmesen JO, Larsen FS, Kondrup J, Hansen BA, Ott P. Cerebral herniation in patients with acute liver failure is correlated with arterial ammonia concentration. *Hepatology* 1999;29:648-653.
11. Shawcross DL, Wright GA, Stadlbauer V, Hodges SJ, Davies NA, Wheeler-Jones C, et al. Ammonia impairs neutrophil phagocytic function in liver disease. *Hepatology* 2008;48:1202-1212.
12. Qiu J, Tsien C, Thalalaya S, Narayanan A, Wehl CC, Ching JK, et al. Hyperammonemia-mediated autophagy in skeletal muscle contributes to sarcopenia of cirrhosis. *Am J Physiol Endocrinol Metab* 2012;303:E983-993.
13. Dasarathy S, Mookerjee RP, Rackayova V, Rangroo Thrane V, Vairappan B, Ott P, et al. Ammonia toxicity: from head to toe? *Metab Brain Dis* 2017;32:529-538.
14. Jalan R, De Chiara F, Balasubramanian V, Andreola F, Khetan V, Malago M, et al. Ammonia produces pathological changes in human hepatic stellate cells and is a target for therapy of portal hypertension. *J Hepatol* 2016;64:823-833.
15. Rombouts K, Marra F. Molecular mechanisms of hepatic fibrosis in non-alcoholic steatohepatitis. *Dig. Dis.* 2010;28:229-235.
16. Ytrebo LM, Kristiansen RG, Maehre H, Fuskevag OM, Kalstad T, Revhaug A, et al. L-ornithine phenylacetate attenuates increased arterial and extracellular brain ammonia and prevents intracranial hypertension in pigs with acute liver failure. *Hepatology* 2009;50:165-174.
17. Kristiansen RG, Rose CF, Fuskevag OM, Maehre H, Revhaug A, Jalan R, et al.

L-Ornithine phenylacetate reduces ammonia in pigs with acute liver failure through phenylacetyl-glycine formation: a novel ammonia-lowering pathway. *Am J Physiol Gastrointest Liver Physiol* 2014;307:G1024-1031.

18. Wright G, Vairappan B, Stadlbauer V, Mookerjee RP, Davies NA, Jalan R. Reduction in hyperammonaemia by ornithine phenylacetate prevents lipopolysaccharide-induced brain edema and coma in cirrhotic rats. *Liver Int* 2012;32:410-419.
19. Jover-Cobos M, Noiret L, Lee K, Sharma V, Habtesion A, Romero-Gomez M, et al. Ornithine phenylacetate targets alterations in the expression and activity of glutamine synthase and glutaminase to reduce ammonia levels in bile duct ligated rats. *J Hepatol* 2014;60:545-553.
20. Ventura-Cots M, Arranz JA, Simon-Talero M, Torrens M, Blanco A, Riudor E, et al. Safety of ornithine phenylacetate in cirrhotic decompensated patients: an open-label, dose-escalating, single-cohort study. *J Clin Gastroenterol* 2013;47:881-887.
21. Jover-Cobos M, Khetan V, Jalan R. Treatment of hyperammonemia in liver failure. *Curr Opin Clin Nutr Metab Care* 2014;17:105-110.
22. Gutierrez-de-Juan V, Lopez de Davalillo S, Fernandez-Ramos D, Barbier-Torres L, Zubiete-Franco I, Fernandez-Tussy P, et al. A morphological method for ammonia detection in liver. *PLoS One* 2017;12:e0173914.
23. Varghese F, Bukhari AB, Malhotra R, De A. IHC Profiler: an open source plugin for the quantitative evaluation and automated scoring of immunohistochemistry images of human tissue samples. *PLoS One* 2014;9:e96801.
24. Kleiner DE, Brunt EM, Van Natta M, Behling C, Contos MJ, Cummings OW, et al. Design and validation of a histological scoring system for nonalcoholic fatty liver disease. *Hepatology* 2005;41:1313-1321.
25. Calvaruso V, Burroughs AK, Standish R, Manousou P, Grillo F, Leandro G, et al. Computer-assisted image analysis of liver collagen: relationship to Ishak scoring and hepatic venous pressure gradient. *Hepatology* 2009;49:1236-1244.
26. Gracia-Sancho J, Lavina B, Rodriguez-Vilarrupla A, Garcia-Caldero H, Bosch J, Garcia-Pagan JC. Enhanced vasoconstrictor prostanoid production by sinusoidal endothelial cells increases portal perfusion pressure in cirrhotic rat livers. *J Hepatol* 2007;47:220-227.
27. de Mesquita FC, Guixe-Muntet S, Fernandez-Iglesias A, Maeso-Diaz R, Vila S, Hide D, et al. Liraglutide improves liver microvascular dysfunction in cirrhosis: Evidence from translational studies. *Sci Rep* 2017;7:3255.
28. Jalan R, Wright G, Davies NA, Hodges SJ. L-Ornithine phenylacetate (OP): a novel treatment for hyperammonemia and hepatic encephalopathy. *Med Hypotheses* 2007;69:1064-1069.
29. Paish HL, Reed LH, Brown H, Bryan MC, Govaere O, Leslie J, et al. A Bioreactor Technology for Modeling Fibrosis in Human and Rodent Precision-Cut Liver Slices. *Hepatology* 2019.
30. Gips CH, Wibbens-Alberts M. Ammonia determination in blood using the TCA direct method. *Clin Chim Acta* 1968;22:183-186.
31. Buckner JC, Malkin MG, Reed E, Cascino TL, Reid JM, Ames MM, et al. Phase II study of antineoplastons A10 (NSC 648539) and AS2-1 (NSC 620261) in patients with recurrent glioma. *Mayo Clin Proc* 1999;74:137-145.
32. Govaere O, Reed LH, Brown H, Cockell SJ, French JJ, White SA, et al. Precision-cut liver slices as an ex-vivo model for human NAFLD show hepatic progenitor cell activation and fibrogenesis. Abstract, The International Liver Congress. 2017.
33. Charbonneau R, Roberge A, Berlinguet L. Variation with age of the enzymes of the urea cycle and aspartate transcarbamylase in rat liver. *Can J Biochem* 1967;45:1427-

1432.

34. Rock KL, Kono H. The inflammatory response to cell death. *Annu Rev Pathol* 2008;3:99-126.

35. Venereau E, Ceriotti C, Bianchi ME. DAMPs from Cell Death to New Life. *Front Immunol* 2015;6:422.

36. Dadsetan S, Sorensen M, Bak LK, Vilstrup H, Ott P, Schousboe A, et al. Interorgan metabolism of ornithine phenylacetate (OP)--a novel strategy for treatment of hyperammonemia. *Biochem Pharmacol* 2013;85:115-123.

37. Lee YH, Kim SU, Song K, Park JY, Kim DY, Ahn SH, et al. Sarcopenia is associated with significant liver fibrosis independently of obesity and insulin resistance in nonalcoholic fatty liver disease: Nationwide surveys (KNHANES 2008-2011). *Hepatology* 2016;63:776-786.

TABLES

Table 1. Clinical and biochemical characteristics of the animal models

	4 weeks			p value	10 weeks			p value	16 weeks			p value
	Normal chow n=5	HC diet n=5	HFHC diet n=5		Normal chow n=5	HC diet n=5	HFHC diet n=5		Normal chow n=5	HC diet n=5	HFHC diet n=5	
Whole BW, start (g)	228 (225-229)	230 (228-238)	220 (212-233)	0.32	230 (221-240)	212 (209-221)	234 (220-235)	0.26	233 (227-233)	222 (211-226)	236 (222-255)	0.16
Whole BW, end (g)	336 (320-338)	358 (355-410)*	387 (387-406)*	0.009	446 (438-475)	492 (486-521)	470 (464-483)	0.20	533 (529-578)	498 (488-512)	513 (499-513)	0.29
Weight gain (g)	109 (100-111)	136 (127-166)*	173 (167-177)*	0.006	212 (208-225)	265 (252-309)	245 (230-252)	0.10	313 (296-345)	290 (262-295)	277 (264-291)	0.47
Liver weight (g)	7 (7-7)	13 (12-16)*	21 (20-21)*	0.002	15 (15-16)	18 (17-19)*	20 (20-20)*##	0.002	17 (15-18)	21 (19-22)**	36 (33-38)*#	0.003
Liver/body weight	2.1 (1.9-2.2)	3.6 (3.2-3.7)*	5.2 (5.1-5.4)*	0.002	3.4 (3.3-3.6)	3.5 (3.3-3.9)	4.4 (4.0-4.7)*##	0.02	2.9 (2.8-3.2)	3.8 (3.7-4.6)*	6.7 (6.5-7.4)*#	0.002
ALT (U/L)	33 (31-35)	23 (22-24)*	76 (66-159)*##	0.003	34 (34-38)	31 (30-34)	310 (275-340)*#	0.008	57 (53-59)	31 (27-43)**	136 (127-153)*##	0.004
AST (U/L)	66 (62-66)	63 (58-76)	126 (109-214)*#	0.009	66 (63-74)	97 (86-123)**	597 (486-600)*##	0.005	120 (103-218)	93 (76-111)	219 (178-227)#	0.03
Bilirubin (μmol/L)	0.6 (0.3-0.7)	0.9 (0.6-1.0)	0.7 (0.4-0.7)	0.22	1.3 (1.3-1.4)	0.9 (0.6-1.0)	1.6 (0.8-1.7)	0.34	1.2 (1.1-1.2)	0.8 (0.8-1.4)	0.9 (0.8-1.3)	0.54
Albumin (g/L)	35 (33-37)	35 (35-36)	35 (34-36)	0.99	35 (34-35)	36 (35-37)	34 (34-34)	0.37	33 (33-35)	35 (33-36)	36 (36-37)#	0.04
Total cholesterol (mmol/L)	0.4 (0.4-0.5)	1.3 (1.2-1.3)*	2.6 (2.5-2.7)*##	0.003	1.0 (0.8-1.1)	1.2 (1.1-1.6)	2.0 (1.8-2.1)*##	0.008	1.9 (1.8-3.1)	1.7 (1.4-1.9)	3.4 (3.3-4.8)*##	0.02
Triglyceride (mmol/L)	0.2 (0.1-0.2)	0.3 (0.3-0.3)**	0.4 (0.3-0.4)*	0.009	0.3 (0.2-0.3)	/	/		0.2 (0.2-0.3)	0.3 (0.2-0.4)	0.3 (0.2-0.3)	0.55
Steatosis (0/1/2/3) n	5/0/0/0	5/0/0/0	0/4/1/0*#	0.005	4/1/0/0	1/3/1/0	1/1/3/0	0.09	5/0/0/0	1/4/0/0**	0/0/4/1*##	0.001
Ballooning (0/1/2) n	5/0/0	3/2/0	0/1/4*##	0.005	5/0/0	3/2/0	1/2/2	0.07	3/2/0	0/3/2	0/0/5*##	0.007
Inflammation (0/1/2/3) n	1/4/0/0	3/2/0/0	0/0/1/4*##	0.008	5/0/0/0	4/1/0/0	1/0/4/0*##	0.01	2/3/0/0	3/2/0/0	0/1/3/1	0.07
Fibrosis (0/1/2/3) n	5/0/0/0	5/0/0/0	5/0/0/0	1.00	5/0/0/0	5/0/0/0	2/3/0/0*##	0.02	5/0/0/0	5/0/0/0	0/1/1/3*##	0.02

Data are presented as median (IQR)

*p<0.01 compared with NC

**p<0.05 compared with NC

#p<0.01 compared with HC diet

##p<0.05 compared with HC diet

Body and liver weight, plasma concentrations of alanine aminotransferase (ALT), aspartate aminotransferase (AST), bilirubin, albumin, total cholesterol and triglycerides in normal chow fed animals, high-calorie HC fed animals and high-fat high-cholesterol (HFHC) fed animals after 4, 10 and 16 weeks, respectively.

Table 2. The effect of ornithine phenylacetate on clinical, biochemical and histologic characteristics

	Normal chow			HC diet			HFHC diet			P values comparing all groups
	No treatment n=10	OP treatment n=10	p value	No treatment n=10	OP treatment n=10	p value	No treatment n=10	OP treatment n=10	p value	
Whole BW, start (g)	233 (222-235)	230 (219-232)	/	231 (220-233)	226 (215-228)	/	223 (220-235)	222 (211-224)	/	P=0.18
Whole BW, end (g)	548 (525-578)	573 (541-577)	/	588 (545-632)	593 (546-610)	/	548 (513-579)	592 (531-611)	/	P=0.37
Weight gain (g)	327 (296-345)	335 (311-359)	/	362 (302-401)	371 (321-386)	/	325 (282-344)	372 (322-395)	/	P=0.22
Liver weight (g)	17 (16-19)	16 (13-17)	0.17	19 (16-22)	16 (14-18)	0.05	33 (31-34)	33 (31-35)	0.94	P=0.0001
Liver/body weight	3.2 (2.8-3.2)	2.8 (2.7-3.0)	0.02	3.1 (3.1-3.5)	2.8 (2.4-3.0)	0.003	6.2 (5.9-6.2)	5.5 (5.4-5.8)	0.04	P=0.0001
ALT (U/L)	54 (51-58)	40 (35-53)	0.08	106 (32-128)	52 (28-66)	0.11	135 (79-190)	113 (82-171)	0.94	P=0.002
AST (U/L)	95 (80-160)	65 (58-73)	0.01	74 (57-186)	93 (81-168)	0.55	189 (130-381)	218 (170-267)	0.76	P=0.001
Bilirubin (μmol/L)	1.0 (0.7-1.2)	1.1 (0.7-1.4)	/	0.9 (0.6-1.0)	1.3 (0.9-1.7)	/	1.1 (0.8-1.4)	1.0 (0.7-1.1)	/	P=0.30
Albumin (g/L)	33 (31-34)	32 (30-34)	/	33 (31-34)	33 (31-35)	/	32 (31-33)	32 (31-33)	/	P=0.89
Total cholesterol (mmol/L)	1.4 (1.0-1.9)	1.2 (1.1-1.4)	0.55	1.6 (1.4-2.3)	1.5 (1.3-1.7)	0.33	3.3 (1.5-4.9)	2.8 (1.4-3.1)	0.11	P=0.005
Triglyceride (mmol/L)	0.2 (0.2-0.3)	0.3 (0.2-0.4)	0.54	0.3 (0.1-0.4)	0.2 (0.2-0.4)	0.62	0.1 (0.1-0.2)	0.1 (0.0-0.2)	0.10	P=0.002
Steatosis (0/1/2) n	9/1/0	9/1/0	1.00	5/5/0	8/2/0	0.16	0/5/5	0/3/7	0.36	P<0.001
Ballooning (0/1/2) n	4/5/1	8/2/0	0.16	3/6/1	8/1/1	0.05	0/2/8	0/1/9	0.53	P<0.001
Inflammation (0/1/2/3) n	7/3/0/0	6/4/0/0	0.64	8/2/0/0	9/1/0/0	0.53	0/0/7/3	0/0/5/5	0.36	P<0.001
Fibrosis (0/1/2/3) n	10/0/0/0	10/0/0/0	1.00	10/0/0/0	10/0/0/0	1.00	0/0/5/5	0/5/2/3	0.03	P<0.001

Data are presented as median (IQR)

/ indicates that statistical analyses were not performed as no significant difference was found comparing all groups using Kruskal-Wallis rank test

Body and liver weight, plasma concentrations of alanine aminotransferase (ALT), aspartate aminotransferase (AST), bilirubin, albumin, total cholesterol and triglycerides and histology scores in normal chow fed animals, high-calorie HC fed animals and high-fat high-cholesterol (HFHC) fed animals with and without ornithine phenylacetate (OP) treatment.

FIGURE LEGENDS

Figure 1. Progressive urea cycle enzyme dysfunction, hyperammonaemia and fibrosis in the NAFLD animal model

(A) Representative H&E, picro-sirius red (PSR) stain and polarized light (PL) imaging (magnification x10) of liver from controls (NC) and from animals fed a high-calorie HC and a high-fat high-cholesterol (HFHC) diet for 4, 10 and 16 weeks. (B) Collagen deposition in NC, HC and HFHC diet groups. (C) Liver protein expression of collagen type I alpha 1 (Col1A1), Myosin IIa, Myosin IIb and alpha smooth muscle actin (α -SMA) in NC, HC and HFHC animals. The samples from each group were pooled (n=5 livers per group) and presented as columns representing the mean. (D) Hepatic ornithine transcarbamylase (OTC) activity in NC, HC and HFHC animals. (E) Plasma ammonia levels in NC, HC and HFHC animals. (F) Nessler's staining (magnification x10 and x100) confirmed the presence of high levels of ammonia (brown precipitates) in the liver of HFHC group compared with NC and HC at 16 weeks. (G) Plasma histone-associated DNA fragments in NC, HC and HFHC animals. (H) TUNEL staining of the liver tissue (magnification x10 and x100) in NC, HC and HFHC animals. The columns indicate the mean values and the error bars SD.

Figure 2. Progressive hyperammonaemia and activation of hepatic stellate cells (HSCs) in an in vitro model of steatosis

(A) Primary hepatocytes (magnification x10) incubated with free fatty acids (FFAs) showed accumulation of lipid droplets intracellularly by Oil-red-O staining compared with controls (NT) and (B) increased ammonia levels in the medium in a FFAs dose-dependent manner. (C) Increased proliferation was observed in HSCs (magnification x10) treated with ammonia and supernatant from FFA-treated hepatocytes (Hep

Sup) for 72h. (D) HSC alpha smooth muscle actin (α -SMA) and collagen type I alpha 1 (Col1A1) expression at the mRNA level and (E) at the protein level demonstrated by western blots (WB) (pooled samples, n=4 per group) and (F) for α -SMA also by fluorescence staining (magnification x10) in NT-, FFA-, ammonia- and Hep Sup-treated cells. Replacing the FFA, ammonia or Hep Sup medium with serum free medium for another 72h led to amelioration in HSCs phenotype (C-F). (G) Activation of Kupffer cells (KCs) (magnification x10 and x40) was observed after treatment with ammonia or supernatant for 24h. (H) mRNA level of interleukin (IL)-1 β , IL-6, IL-10 and chemokine (C-C motif) ligand 2 (CCL2). The columns indicate the mean values and the error bars SD.

Figure 3. Prevention of progression of hepatic fibrosis in precision cut liver slices (PCLS) after treatment with the ammonia scavenger ornithine phenylacetate (OP)

(A) Albumin and lactate dehydrogenase (LDH) in the culture medium of the liver slices after treatment with free fatty acid (FFA) (2 mM) and/or ammonia (100 μ m) and adding OP (150 μ g/ml) to the culture medium for the last 48 hours. (B) Ammonia levels in the culture medium after 72h and 96 h. (C) Gene expression of alpha smooth muscle actin (α -SMA) and collagen type I alpha 1 (Col1A1) after treatment with free fatty acid (FFA) and/or ammonia and OP at the end of the study. (D) Collagen accumulation in the liver slices defined by picro-sirius red staining after treatment with FFAs and/or ammonia and OP compared to control slices (NT). The columns indicate the mean values and the error bars SD. - indicates no treatment, + indicates treatment with the respective compounds and +/- indicates that half of the slices were treated and the other half was not.

Figure 4. Prevention of progression of hepatic fibrosis in NAFLD animals after treatment with the ammonia scavenger, ornithine phenylacetate (OP)

(A) Ornithine transcarbamylase (OTC) activity in controls (NC), high-calorie HC diet fed and high-fat high-cholesterol (HFHC) diet fed animals +/- OP treatment. (B) Plasma ammonia levels in NC, HC and HFHC-fed animals +/- OP treatment. (C) Ammonia levels in the liver tissue of NC, HC and HFHC-fed animals +/- OP treatment (magnification x10 and x100). (D) Urinary phenylacetylglutamine (PAG) and phenylacetylglutamine PAGN concentrations in controls (NC) and in OP-treated high-calorie HC and high-fat high-cholesterol (HFHC) diet fed animals. (E) Plasma interleukin (IL)-1 β and IL-10 levels in NC, HC and HFHC-fed animals +/- OP treatment. (F) Plasma TLR4-ligand levels in NC, HC and HFHC-fed animals +/- OP treatment. (G) Cell death components in plasma in NC, HC and HFHC-fed animals +/- OP treatment. (H) TUNEL staining of liver tissue (magnification x10 and x100) in NC, HC and HFHC-fed animals +/- OP treatment. (I) Representative H&E, picrosirius red (PSR) stain and polarized light (PL) imaging of liver (magnification x10) from HFHC animals +/- OP treatment and fibrosis quantification of all groups. (J) Hepatic protein expression of collagen type I alpha 1 (Col1A1), Myosin IIa, Myosin IIb and alpha smooth muscle actin (α -SMA) in NC, HC and HFHC-fed animals +/- OP treatment. The samples from each group were pooled (n=10 livers per group) and presented as columns representing the mean. For all other figures, the columns indicate the mean values and the error bars SD.

Figure 5. Prevention of progression of fibrosis in NAFLD after treatment with ornithine phenylacetate (OP)

In NAFLD, hepatic and systemic hyperammonaemia is evident due to reduced urea synthesis. Hyperammonaemia activates hepatic stellate cells and Kupffer cells which is associated with progressive hepatic fibrosis. Lowering of ammonia with the ammonia scavenger ornithine phenylacetate (OP) significantly reduced the development of fibrosis and may be a novel approach for the prevention of progression of NAFLD.

Figure 1

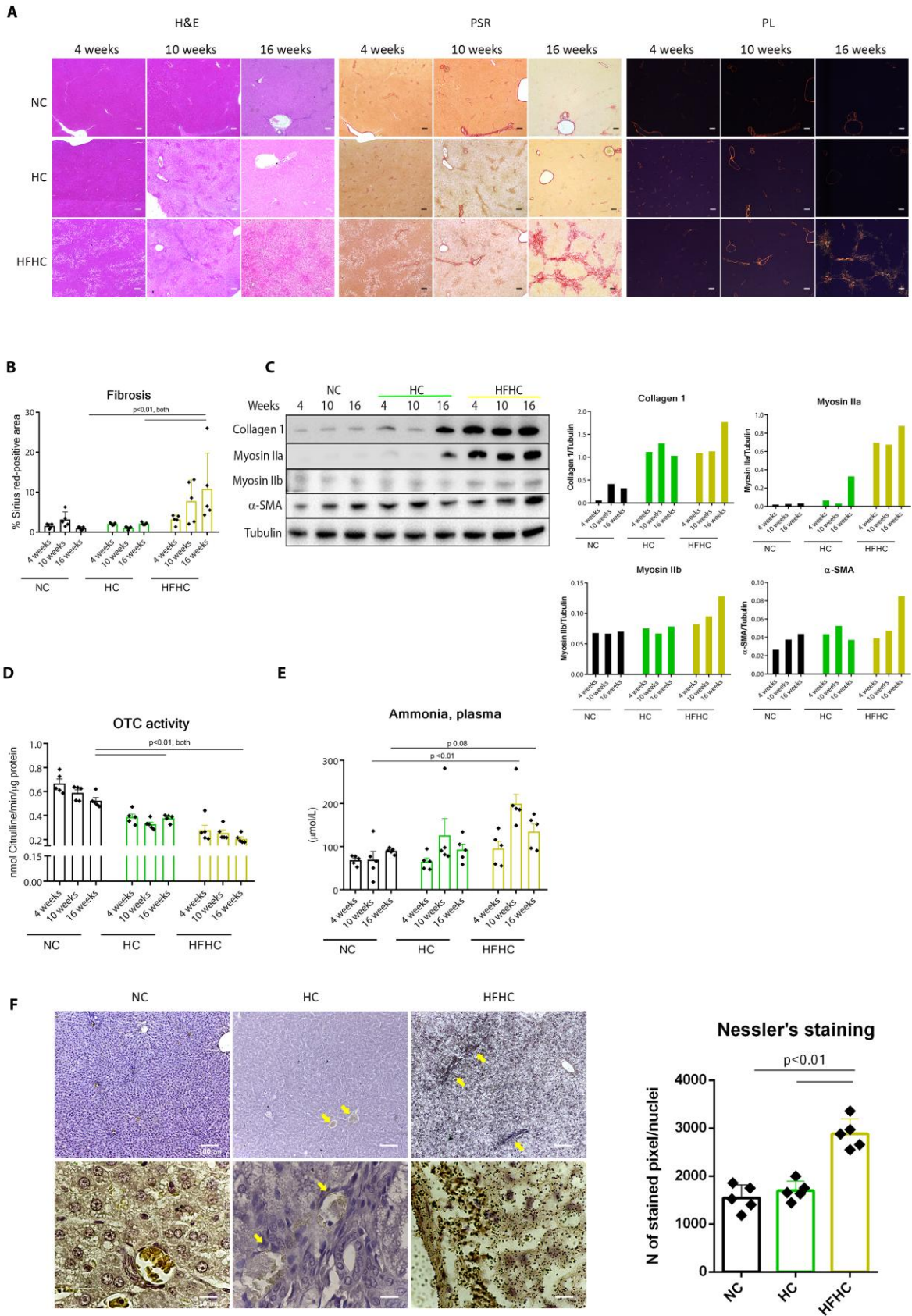


Figure 1

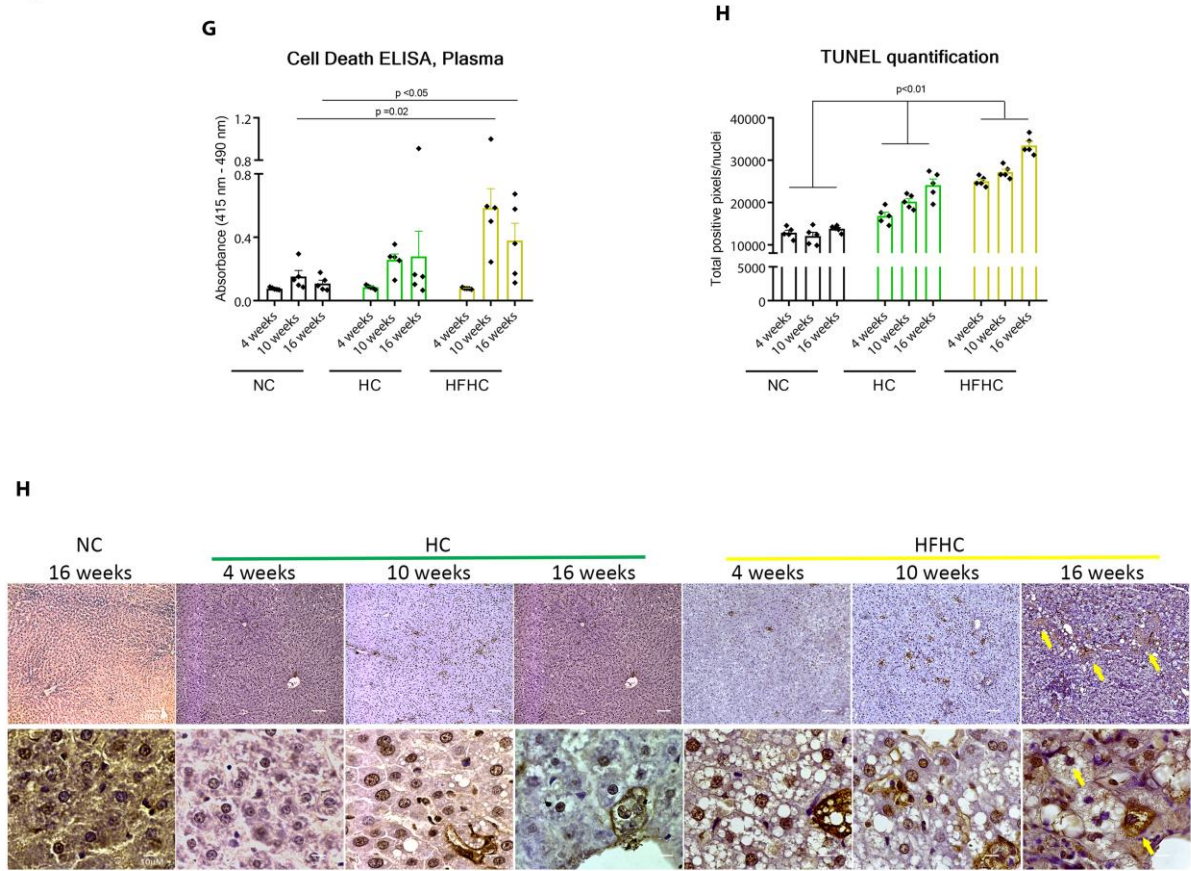


Figure 2

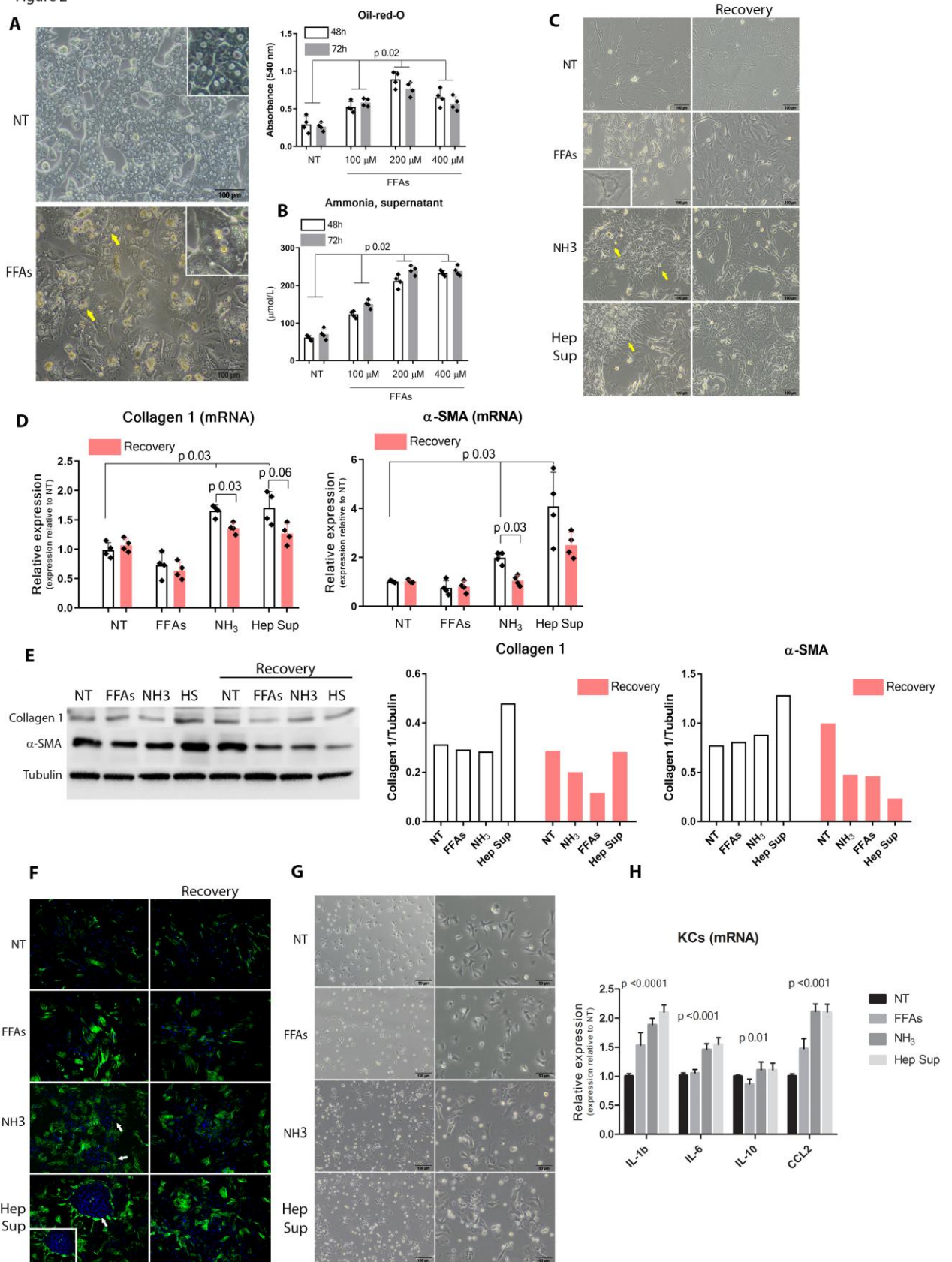


Figure 3

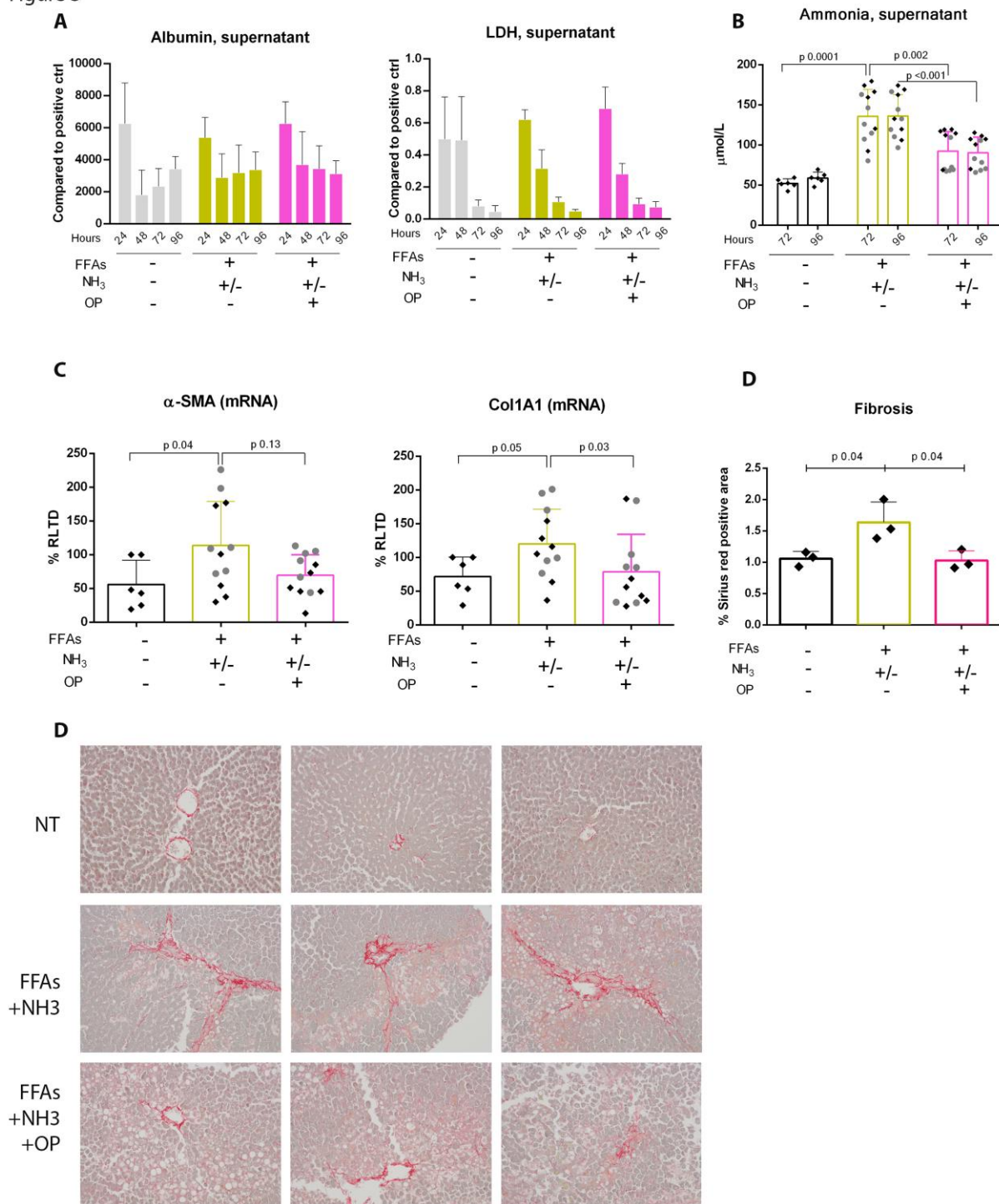


Figure 4

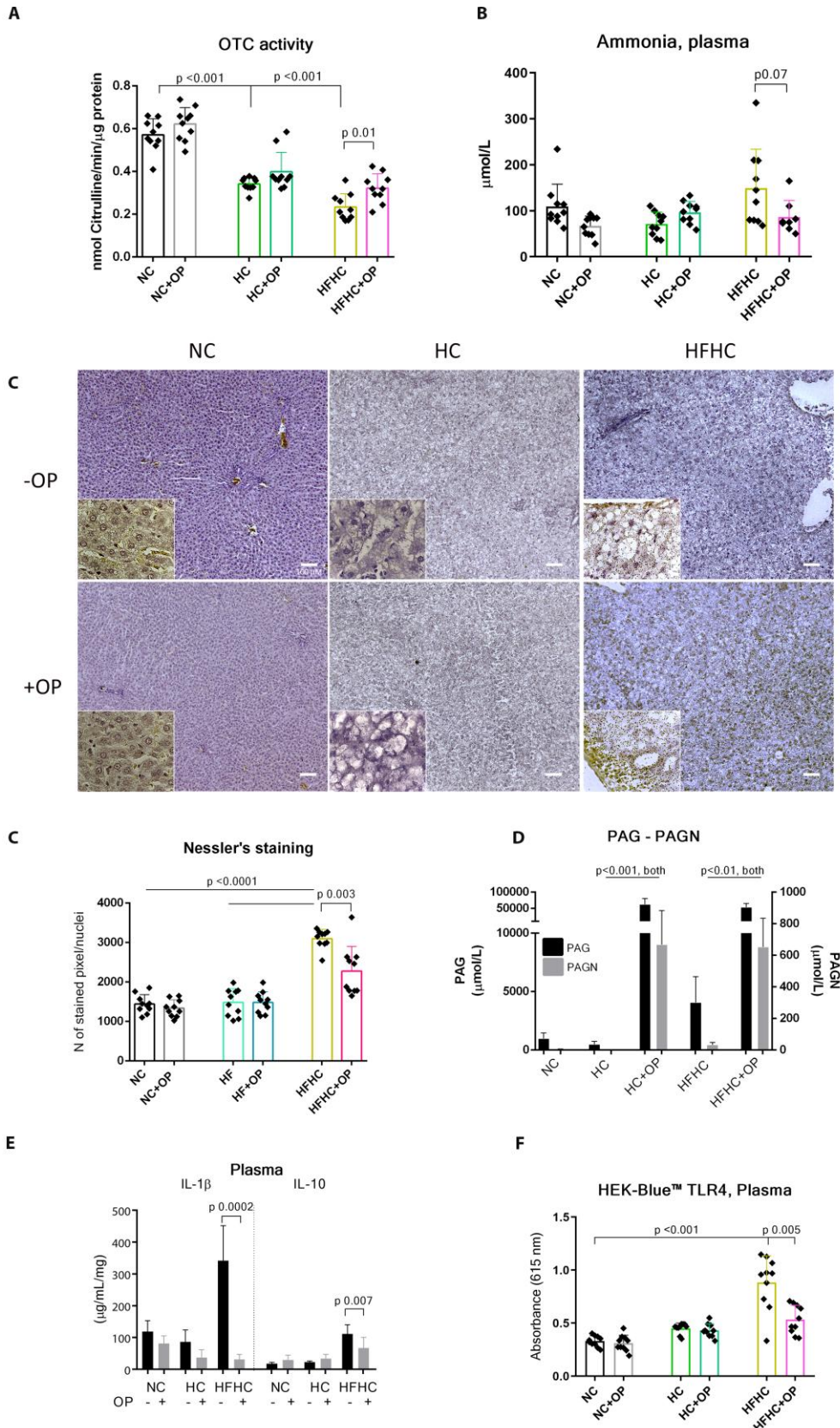


Figure 4

